Ludek Schreier, Jiri Bendl, Miroslav Chomat
Institute of Thermomechanics AS CR, v. v. i., Czechy

NOVEL ARRANGEMENT OF COMBINED STAR-DELTA STATOR WINDING AIMED AT REDUCTION OF COPPER USAGE IN ELECTRIC MACHINE

NOWY UKŁAD UZWOJENIA MIESZANEGO GWIAZDA-TRÓJKĄT W STOJANIE ZMNIEJSZAJĄCY ZUŻYCIE MIEDZI W MASZYNIE ELEKTRYCZNEJ

Abstract: The submitted paper deals with the increased energy efficiency of induction machines by means of the so-called combined stator winding. Two basic variants of this winding, the series and parallel ones, are shown. The suppression of higher harmonics is analysed by means of the method of space vectors and symmetrical components. It is shown that the so-called series variant of the combined winding has a better ability to suppress higher spatial harmonics. The commonly used combined winding has, however, a longer pitch and thus bigger stator resistance and greater consumption of copper. The paper presents a proposal of an adapted combined winding whose pitch is smaller than that of the used three-phase winding. This fact results in decreasing the consumption of copper conductors with preserving the energy efficiency. The results of the analysis have been verified by measurements on physical models of machines with the combined and the adapted combined windings.

1. Introduction

At present, emphasis is put on energy and material consumption all over the world with the aim to ensure sustainable development. Induction motors are the most commonly used type of electric machines. In the literature, considerable attention is paid to increasing their energy efficiency by means of the so-called combined winding [1], [2], and [3]. The advantage of this winding is the ability to suppress higher spatial harmonics and thus improve the efficiency of energy conversion. The usually mentioned types of this winding have, however, a longer pitch of winding than the standard three-phase windings and thus longer ends. This results in increasing winding resistance and in a rise in consumption of copper conductors. The paper will further show a proposal of a combined winding that has shorter ends than a usual three-phase winding and can thus lead to copper savings.

2. Principle of combined winding

The combined stator winding of three-phase induction machines is composed of the delta- and star-connected windings. There are two basic variants of this winding depicted in Fig. 1. In Fig. 1a, there is the so-called series combined winding and in Fig. 1b, there is the so-called parallel variant of the combined winding. With a suitable configuration of the two windings in the space of the machine, higher spatial harmonics of the current layer, induction in the air gap and flux in the yoke produced by the delta- and star-connected windings mutually suppress each other.

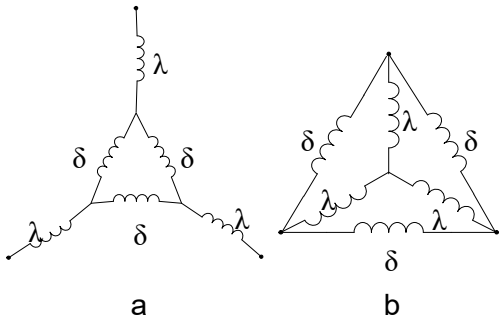

Fig. 1. Basic variants of combined winding.

According to [1], [2], and [4], the harmonics of the order $\nu = 5 + 12k$ and $\nu = 7 + 12k$, where k is a positive integer including 0, can be reduced. These harmonics can be suppressed if two conditions are fulfilled, [1] and [5]. The first condition is that the axes of the star- and delta-connected winding must be mutually shifted by 30 electric degrees, measured in the positive direction from the axis of the delta-connected winding to the axis of the star-connected winding. Under the second condition, the ratio of the conductors of a single phase of the delta-connected winding and the number of the conductors of the star-connected winding must be $\sqrt{3}$. This condition cannot be com-

pletely fulfilled in practice. That is why the harmonics of the higher mentioned orders cannot be entirely eliminated. The mathematical description for the basic harmonic of the series variant, Fig. 1a, is according to [3] given by the system of two differential equations

$$u_\delta = R_{\lambda\delta} i_\delta + L_{\sigma\lambda\delta}\frac{di_\delta}{dt} + (L_{h\lambda} + L_{h\delta} + L_{h\lambda\delta})\left(e^{-j\alpha}e^{j^{\pi/6}} + e^{j\alpha}e^{-j^{\pi/6}}\right)\frac{di_\delta}{dt} + \left(L_{h\lambda\delta}e^{-j\alpha}e^{j^{\pi/6}} + L_{h\delta}\right)\frac{di_{R\lambda\delta}}{dt} \quad (1)$$

and

$$0 = R_{R\delta} i_{R\lambda\delta} + L_{\sigma R\delta}\frac{di_{R\lambda\delta}}{dt} + L_{h\delta}\frac{di_{R\lambda\delta}}{dt} + \left(L_{h\delta} + L_{h\lambda\delta}e^{j\alpha}e^{-j^{\pi/6}}\right)\frac{di_\delta}{dt} - jp\omega_m\left[\begin{matrix} L_{\sigma R\delta} i_{R\lambda\delta} + L_{h\delta} i_{R\lambda\delta} + \\ + \left(L_{h\delta} + L_{h\lambda\delta}e^{j\alpha}e^{-j^{\pi/6}}\right) i_\delta \end{matrix}\right], \quad (2)$$

where $\boldsymbol{u_\delta}$ is the first symmetrical component of the stator line to line voltage, $\boldsymbol{i_\delta}$ is the first symmetrical component of the currents of the delta-connected winding and $\boldsymbol{i_{R\lambda\delta}}$ is the first symmetrical component of the rotor currents rated to the number of the conductors of a single phase of the delta-connected winding and transferred to the stator reference system. Further

$$R_{\lambda\delta} = 3R_\lambda + R_\delta, \quad (3)$$

$$L_{\sigma\lambda\delta} = 3L_{\sigma\lambda} + L_{\sigma\delta}, \quad (4)$$

$$L_{h\lambda\delta} = \frac{3}{2}\sqrt{3}\kappa_\lambda\kappa_\delta N_\lambda N_\delta L_1, \quad (5)$$

$$L_{h\lambda} = \frac{9}{2}(\kappa_\lambda N_\lambda)^2 L_1, \quad (6)$$

$$L_{h\delta} = \frac{3}{2}(\kappa_\delta N_\delta)^2 L_1, \quad (7)$$

$$R_{R\delta} = R_R\frac{3}{m_R}\frac{(\kappa_\delta N_\delta)^2}{(\kappa_R N_R)^2}, \quad (8)$$

$$L_{\sigma R\delta} = L_{\sigma R}\frac{3}{m_R}\frac{(\kappa_\delta N_\delta)^2}{(\kappa_R N_R)^2}, \quad (9)$$

where R_λ and $L_{\sigma\lambda}$ are resistance and leakage inductance of the star-connected winding, R_δ and $L_{\sigma\delta}$ are resistance and leakage inductance of the delta-connected winding, κ_δ, κ_λ, κ_R, N_λ, N_δ and N_R are winding factors and numbers of conductors of the star- and delta-connected windings and of the rotor, R_R and $L_{\delta R}$ are rotor resistance and leakage inductance. The symbol m_R represents the number of rotor phases. In the case of the cage winding, m_R equals the number of bars and N_R equals 1. The shift of the axes of the star- and delta-connected windings is given by angle α. The symbol L_1 is according to [5] and [6] inductance of a single conductor. The torque produced by the delta-connected winding is

$$T_\delta = 6pL_{h\delta}Re[ji_\delta^* i_{R\lambda\delta}]. \quad (10)$$

The torque produced by the star-connected winding is

$$T_\lambda = 6pL_{h\lambda\delta}Re[ji_\delta^* i_{R\lambda\delta}e^{-j\alpha}e^{j^{\pi/6}}]. \quad (11)$$

The resulting torque T is given by the sum of the torques T_δ and T_λ. The motion equation was used in the form

$$\frac{\omega_m}{dt} = \frac{1}{J}(T - T_l), \quad (12)$$

where J is the moment of inertia and T_l is the load torque.

The situation in the machine with a stator parallel winding according to Fig. 1b was analysed in detail in [5]. The result of the analysis has been a system of three differential equations for the star- and delta-connected windings, and the rotor.

$$u_{\lambda\delta} = R_{\lambda\delta} i_{\lambda\delta} + L_\lambda\frac{di_{\lambda\delta}}{dt} + L_h\frac{di_\delta}{dt} + L_h\frac{di_{R\lambda\delta}}{dt}, \quad (13)$$

$$u_\delta = R_\delta i_\delta + L_\delta\frac{di_\delta}{dt} + L_h\frac{di_{\lambda\delta}}{dt} + L_h\frac{di_{R\lambda\delta}}{dt}, \quad (14)$$

$$0 = R_{R\delta} i_{R\lambda\delta} + L_{R\delta}\frac{di_{R\lambda\delta}}{dt} + L_h\frac{di_\delta}{dt} + L_h\frac{di_{\lambda\delta}}{dt} - j\omega_m(L_{R\delta} i_{R\lambda\delta} + L_h i_\delta + L_h i_{\lambda\delta}), \quad (15)$$

where $\boldsymbol{u_{\lambda\delta}}$ and $\boldsymbol{i_{\lambda\delta}}$ are the first symmetrical components of star-connected winding voltage and currents rated to the number of delta-connected winding conductors. Further

$$L_h = \frac{3}{2}(\kappa_\delta N_\delta)^2 L_1, \quad (16)$$

$$R_{\lambda\delta} = R_\lambda\left(\frac{\kappa_\delta N_\delta}{\kappa_\lambda N_\lambda}\right)^2, \quad (17)$$

$$L_{\sigma\lambda\delta} = L_{\sigma\lambda}\left(\frac{\kappa_\delta N_\delta}{\kappa_\lambda N_\lambda}\right)^2, \quad (18)$$

$$L_\lambda = L_{\sigma\lambda\delta} + L_h, \quad (19)$$

$$L_\delta = L_{\sigma\delta} + L_h, \quad (20)$$

$$L_{R\delta} = L_{\sigma R\delta} + L_h. \quad (21)$$

The inductances L_λ and L_δ are given by the sum of the main inductance L_h and the corresponding leakage inductance. The torques generated by the star- and delta-connected windings are in this case

$$T_\lambda = 6pL_h Re[ji_{\lambda\delta}^* i_{R\lambda\delta}], \quad (22)$$

$$T_\delta = 6pL_h Re[ji_\delta^* i_{R\lambda\delta}]. \quad (23)$$

It is obvious from the different mathematical descriptions that the two variants of the combined winding have different properties. In the case of the parallel combined winding, there must also be, besides the two above mentioned conditions, fulfilled further conditions so that the spatial harmonics of the above mentioned orders are eliminated. The main inductance of the star- and delta-connected windings given by equations (6) and (7) must have the same value and the ratio of the resistances and leakage inductances of the star- and delta-connected

windings must also equal $\sqrt{3}$. Neither this can be fulfilled precisely in practice. Mainly for this reason, the variant of the series connection of the combined winding better suppress higher spatial harmonics and therefore, the attention will be further paid to it.

3. Arrangement of winding in slots

The example of the arrangement of a stator combined winding of a two-pole machine with 24 slots is shown in Figs. 2 and 3.

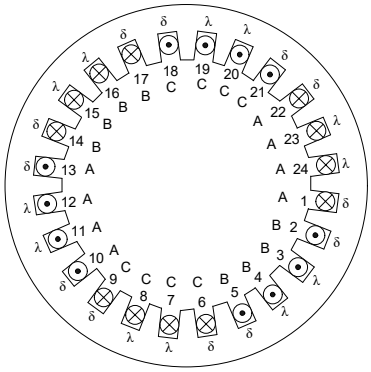

Fig. 2. Spatial arrangement of combined winding

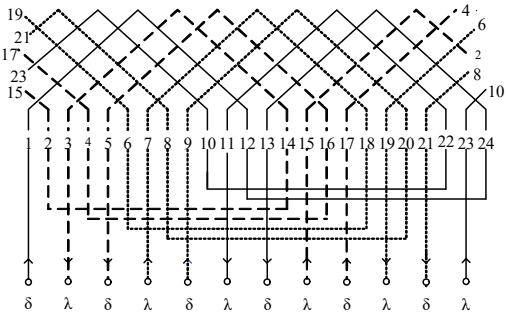

Fig. 3. Scheme of combined winding

Figure 2 shows the arrangement of the combined diamond winding in the space of the machine. The scheme of the connection of this winding is in Fig. 3. The winding of the phase *A* is depicted by the solid line, the winding of the phase *B* by the dashed line and the winding of the phase *C* by the dotted line. This winding can also be proposed as a concentric winding. It is obvious from the two figures that the pitch of the delta- and star-connected windings is 11 slots. For comparison, the spatial arrangement and the scheme of the connection of the commonly used three-phase diamond winding is shown in Figs. 4 and 5.

It is evident that the pitch of the three-phase winding is 10 slots. The combined winding has longer ends and thus a greater length of individual coils, greater consumption of copper and bigger resistance.

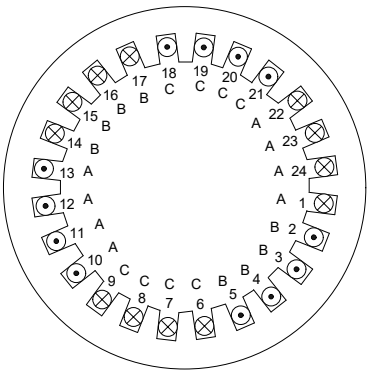

Fig. 4. Spatial arrangement of three-phase winding

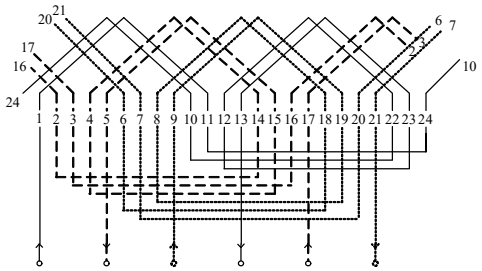

Fig. 5. Scheme of three-phase winding

It is evident that the pitch of the three-phase winding is 10 slots. The combined winding has longer ends and thus a greater length of individual coils, greater consumption of copper and bigger resistance. Combined winding can be adapted according to Figs. 6 and 7.

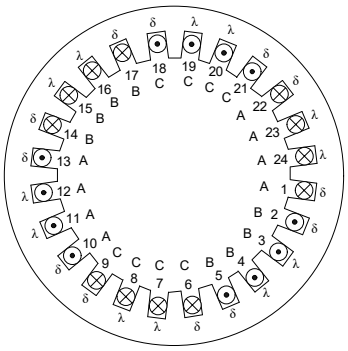

Fig. 6. Spatial arrangement of adapted combined winding

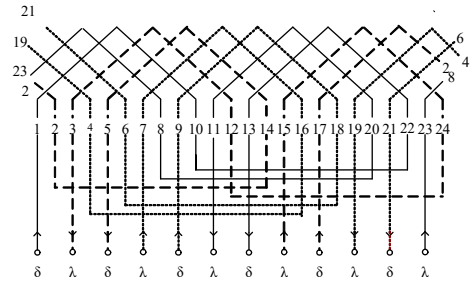

Fig. 7. Scheme of three-phase winding

It is obvious from Figs. 6 and 7 that the pitch of the adapted combined winding is 9 slots. This winding has thus shorter ends and bigger resistance than the usual three-phase winding.

4. Comparison of properties of individual winding configurations

The significant property of machines with the combined winding is their ability to suppress higher spatial harmonics of the above mentioned orders. The factors of the combined winding as well as the adapted combined winding have for some spatial harmonics values that are bigger that the magnitudes of the factors of the three-phase winding. The factors of the winding of the waves of the orders 1 to 13 are in Table 1.

Table 1

Winding	ν=1	ν=5	ν=7	ν=11	ν=13
3-phase	0.957	0.205	0.157	0.126	0.126
Comb.	0.991	0.793	0.608	0.130	0.130
Adapted	0.923	0.382	0.923	0.382	0.382

The reduction of higher spatial harmonics of considered orders is clearly apparent from the waveforms of the so-called current waves, which are proportional to the harmonics of the current layer along the air gap. The current layer of the ν-th current wave of the delta-connected winding is

$$\boldsymbol{l}_{N\delta\nu} = \kappa_{\delta\nu} N_\delta (i_{A\delta} + \boldsymbol{a}^{\nu} i_{B\delta} + \boldsymbol{a}^{2\nu} i_{C\delta}). \quad (24)$$

As the star-connected winding is shifted by α, the current layer of this winding is

$$\boldsymbol{i}_{N\lambda\nu} = \kappa_{\lambda\nu} N_\lambda (i_{A\lambda} + \boldsymbol{a}^{\nu} i_{B\lambda} + \boldsymbol{a}^{2\nu} i_{C\lambda}) e^{j\nu\alpha}. \quad (25)$$

The final stator vector $\boldsymbol{i}_{N\nu}$ is given by the sum of the vectors $\boldsymbol{i}_{N\lambda\nu}$ and $\boldsymbol{i}_{N\delta\nu}$. By means of the simulation model set up on the basis of the derived equations, the phase currents of the corresponding The final stator vector $\boldsymbol{i}_{N\nu}$ is given by the sum of windings from which the mentioned current waves can be determined have been evaluated.

Simulations have been carried out for parameters of experimental machines derived from the commonly used two-pole three-phase machine with the nominal output of 600 W. The stator winding of this machine is shown in Figs. 4 and 5. The experimental machines were produced in cooperation with ATAS elektromotory Náchod, a.s. The star-connected winding has 92 conductors in a slot, the delta-connected winding has 159 conductors in a slot. The main parameters of machines with combined windings according Figs. 2 and 3 are: $R_\lambda = 6.8\ \Omega$, $R_\delta = 19.6\ \Omega$, $X_{\sigma\lambda} = 2.73\ \Omega$, and $X_{\sigma\delta} = 8.17\ \Omega$. The main reactance of the star-connected winding $X_{h\lambda} = 62.96\ \Omega$, the mane of the delta-connected winding is $X_{h\delta} = 188.06\ \Omega$. The resistance of the rotor winding rated to the number of conductors of the delta-connected winding $R_{R\delta} = 8.11\ \Omega$ and the leakage reactance $X_{\sigma R\delta} = 11.60\ \Omega$. The main parameters of the adapted combined winding according Figs. 6 and 7 are: $R_\lambda = 5.5\ \Omega$, $R_\delta = 16.16\ \Omega$, $X_{\sigma\lambda} = 2.73\ \Omega$, $X_{\sigma\delta} = 8.17\ \Omega$, $X_{h\lambda} = 54.68\ \Omega$, $X_{h\delta} = 163.33\ \Omega$, $R_{R\delta} = 7.13\ \Omega$, $X_{\sigma R\delta} = 10.08\ \Omega$.

The waveforms of the real part (solid line) and of the imaginary part (dashed line) of the vectors $\boldsymbol{i}_{N\lambda1}$, $\boldsymbol{i}_{N\delta1}$ and $\boldsymbol{i}_{N1}$ of the series combined stator winding stator are shown in Fig. 8. The same waveforms but for ν = 7 are shown in Fig. 9.

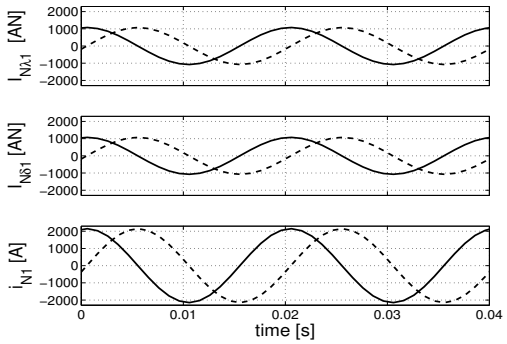

Fig. 8. Series combined winding, vectors $\boldsymbol{i}_{N\lambda1}$, $\boldsymbol{i}_{N\delta1}$ *and* $\boldsymbol{i}_{N1}$

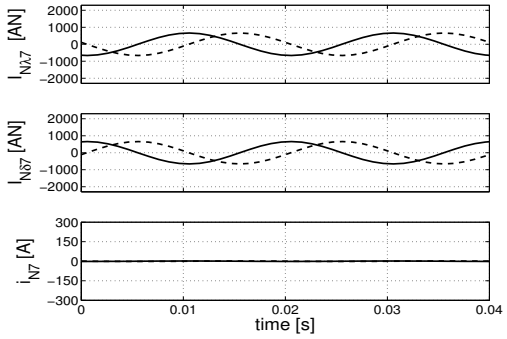

Fig. 9. Series combined winding, vectors $\boldsymbol{i}_{N\lambda7}$, $\boldsymbol{i}_{N\delta7}$ *and* $\boldsymbol{i}_{N7}$

The waveforms of the real and imaginary parts of the vector of the current wave of the fundamental harmonic for the parallel connection of the combined winding are shown in Fig. 10 and for ν = 7 are shown in Fig. 11. The calculations have been carried out for the load torque $T_l = 2.1$ Nm. It is obvious from the figures that the parallel combined winding has a slightly smaller ability to suppress higher

harmonic waves. For this reason, attention will be further paid in the case of the adapted combined winding only to the series connection.

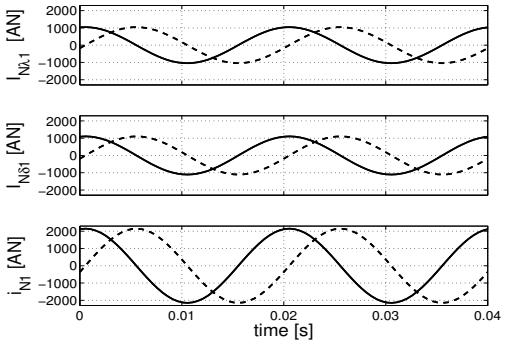

Fig. 10. Parallel combined winding, vectors $\boldsymbol{i}_{N\lambda 1}$, $\boldsymbol{i}_{N\delta 1}$ *and* $\boldsymbol{i}_{N1}$

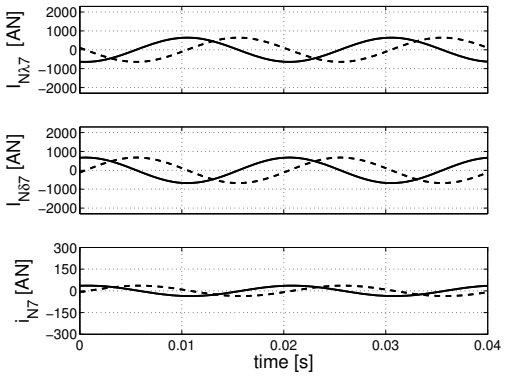

Fig. 11. Parallel combined winding, vectors $\boldsymbol{i}_{N\lambda 7}$, $\boldsymbol{i}_{N\delta 7}$ *and* $\boldsymbol{i}_{N7}$

Figures 12, and 13 show the waveforms of real and imaginary parts of vectors of current waves of individual windings and the final vector of the basic wave and the wave of the order ν = 7. Though the wave of the order ν = 7 has the same winding factor as the basic wave (see Table 1), it is almost entirely suppressed by the adapted combined winding.

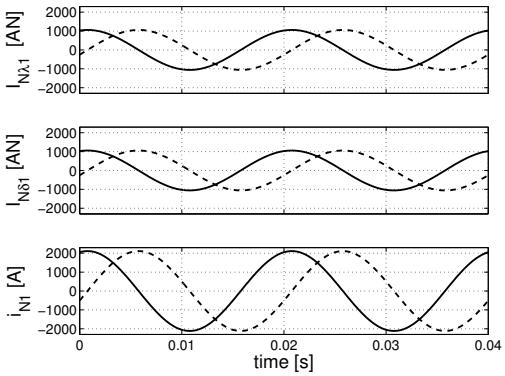

Fig. 12. Series adapted winding, vectors $\boldsymbol{i}_{N\lambda 1}$, $\boldsymbol{i}_{N\delta 1}$ *and* $\boldsymbol{i}_{N1}$

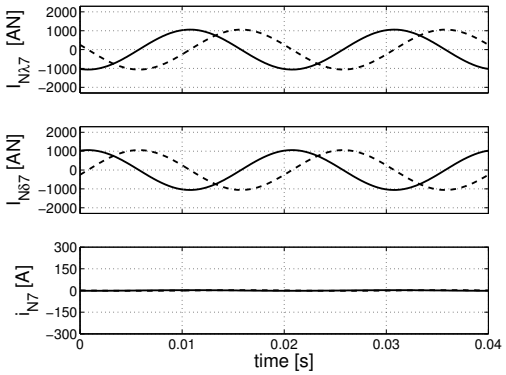

Fig. 13. Series adapted winding, vectors $\boldsymbol{i}_{N\lambda 7}$, $\boldsymbol{i}_{N\delta 7}$ *and* $\boldsymbol{i}_{N7}$

The waves of orders $\nu = 5 + 12\,k$ and $\nu = 7 + 12\,k$, are suppressed similarly as the seventh waves.

5. Experimental verification

To verify the obtained theoretical conclusions, the simulated and measured waveforms of the stator currents of the experimental machines with the combined winding were compared. Figure 14 shows the measured phase voltage of the phase *A* of the source and the measured current of the phase *A* flowing to the machine. Figure 15 depicts simulated waveforms of the currents of the phase *A* of the delta- and star-connected windings and the voltage. The current of the star-connected winding is in fact the current flowing from the source to the motor. The measurements and the calculations were carried out for no-load operation at a speed of 3000 rpm.

The magnitude of the simulated current as well as its phase shift towards the voltage corresponds to the measured values. The same quantities as in Figs. 17 and 18, but for the machine with the adapted combined winding, are shown in Figs. 16 and 17.

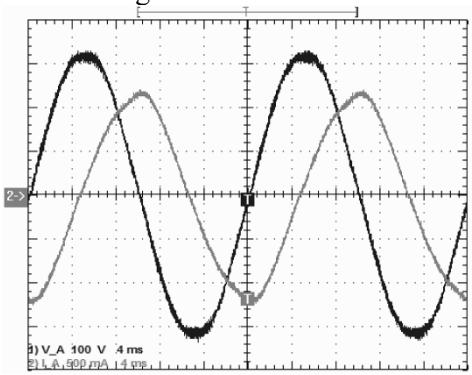

Fig. 14. Combined winding, measured voltage and current

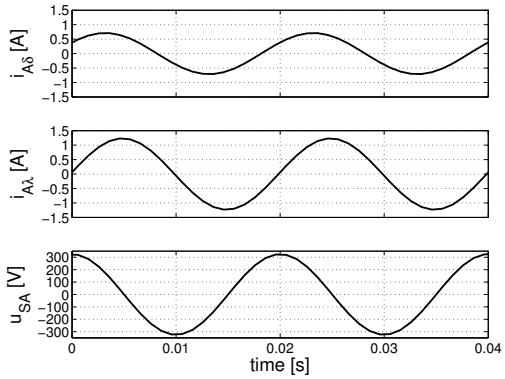

Fig. 15. Combined winding, simulated voltage and currents

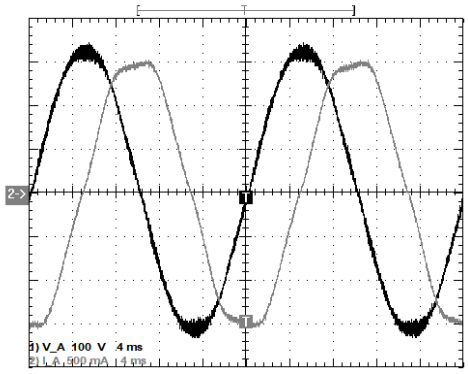

Fig. 16. Adapted winding, measured voltage and current

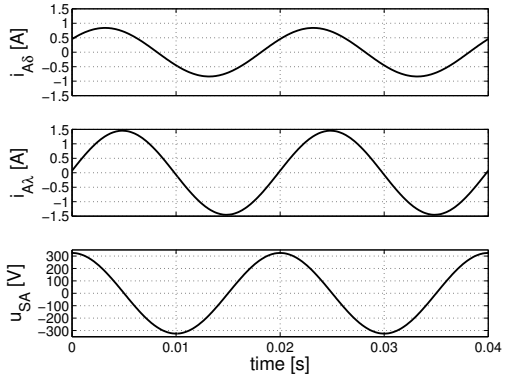

Fig. 17. Adapted winding, simulated voltage and currents

The agreement between the simulated and measured waveforms of currents is very good.

6. Conclusions

The winding of the machine with the combined winding and of a conventional three-phase machine have different pitches. The pitch of the combined winding is 11 slots, while the pitch of the three-phase winding is 10 slots. For this reason the resistance of the combined winding is bigger approximately by 7.5 %. The pitch of the adapted combined winding is 9 slots. The resistance of the winding decreased in this case by 7.2 % in comparison with the three-phase machine. The decrease in resistance is proportional to the length of the used conductors and thus represents significant copper savings. The measurement has proved that the suppression of higher harmonics both in the case of the combined and the adapted combined windings resulted in greater energy efficiency during the operation with the nominal torque approximately by 0.6 %.

7. Bibliography

[1]. Kasten H., Hofmann W.: *Electrical Machines with Higher Efficiency through Combined Star-Delta Windings.* Proc. of IEEE International Electric Machines and Drives Conference. 2011, pp. 1374-1379.

[2]. Raziee S.M., Misir O., Ponick B.: *Combined Star-Delta Winding Analysis*. IEEE Transaction on Energy Conversion. 2017, pp. 1-12.

[3]. Schreier L., Bendl J., Chomat M.: *Analysis of Induction Machines with Combined Stator Windings*. Acta Technica vol. 60, 2015, pp. 155-171.

[4]. Schreier L., Bendl J., Chomat M.: *Effect of combined stator winding on reduction of higher spatial harmonics in induction machine*. Electrical Engineering 10, 2016, pp. 1-9.

[5]. Schreier L, Bendl J., Chomat M.: *Analysis of Properties of Induction Machine with Combined Parallel Star-Delta Stator Winding.* Maszyny Elektryczne-Zeszyty Problemowe 1. 2017, pp 147-153.

[6]. Stepina J.: *Fundamental Equations of the Space Vector Analysis of Electrical Machines*. Acta Technica CSAV (6), 1968, pp.184-198.

Acknowledgement

This work was supported by the Grant Agency of the Czech Republic under research grant No. 16-07795S and by the institutional support RVO 61388998.

Authors

Ludek Schreier, Jiri Bendl, Miroslav Chomat
Institute of Thermomechanics, AS CR, v.v.i.
Department of Electrical Engineering and Electrophysics
Dolejskova 5
18200 Prague 8, Czech Republic
e-mail: schreier@it.cas.cz, bendl@it.cas.cz, chomat@it.cas.cz